JOURNAL OF SOLID STATE CHEMISTRY 52, 138–145 (1984)

The Crystal and Magnetic Structures of Sr_2YRuO_6

P. D. BATTLE* AND W. J. MACKLIN

Inorganic Chemistry Laboratory, South Parks Road, Oxford OX1 3QR, England

Received August 12, 1983

Time-of-flight powder neutron diffraction data have been used to refine the crystal structure of the ordered, distorted perovskite Sr_2YRuO_6. Yttrium and ruthenium are octahedrally coordinated in this material with average M–O bond lengths of 2.202 and 1.955 Å, respectively. Constant wavelength neutron diffraction data show that Sr_2YRuO_6 is a Type I antiferromagnet at 4.2 K with an ordered magnetic moment of 1.85 μ_B per Ru^{5+} ion. The Néel temperature of Sr_2YRuO_6 was determined to be 26 K. The data suggest that the $4d^3$ electrons in this material are localized rather than itinerant.

Introduction

We have undertaken a structural and magnetic study of the compounds in the series $M_2^{II}Ln^{III}Ru^{V}O_6$ (M = Ca, Sr, Ba; Ln = La, Y) which adopt a perovskite-like structure with an ordered arrangement of pentavalent ruthenium and one other cation species on the octahedral (B and B') sites. Our earlier studies on Ba_2LaRuO_6 and Ca_2LaRuO_6 (*1*) have shown that lanthanum occupies an octahedral site in the former material, with an unusually short La–O bond length of ~2.34 Å, whereas the smaller calcium ion drives the lanthanum onto the 12-coordinate A site in Ca_2LaRuO_6. This compound would thus be better described as CaLa[CaRu]O_6 where the brackets enclose the B- and B'-site cations. Both of these materials consist of a $BB'O_6$ framework made up of nearly regular octahedra which are tilted away from their ideal, cubic orientation (Fig. 1). The degree of tilting decreases as the size of the A-site cation increases although the crystal symmetry is lower (triclinic) in Ba_2LaRuO_6 than it is in Ca_2LaRuO_6 (monoclinic). Greatrex *et al.* (*2*) showed that many of these materials order magnetically at low temperatures (<30 K). Magnetic ordering is unusual among compounds containing highly charged cations from the second transition series and these materials offer a rare opportunity to study the magnetic behavior of a $4d^3$ electron system. Our results on Ba_2LaRuO_6 and Ca_2LaRuO_6 were interpreted within a model which assumed the $4d$ electrons to be itinerant but strongly correlated and the two materials were consequently placed in the region $b_c < b < b_m$ on the conceptual temperature vs transfer-integral phase diagram reproduced in Fig. 2. The Type I magnetic ordering found in Ca_2LaRuO_6 indicates that nearest-neighbor superexchange is the only significant magnetic interaction in this material, whereas the Type IIIa ordering found in Ba_2LaRuO_6 indicates that the next-nearest-neighbor interaction, although weaker than that between nearest neighbors, is not negligible

* To whom correspondence should be addressed.

0022-4596/84 $3.00

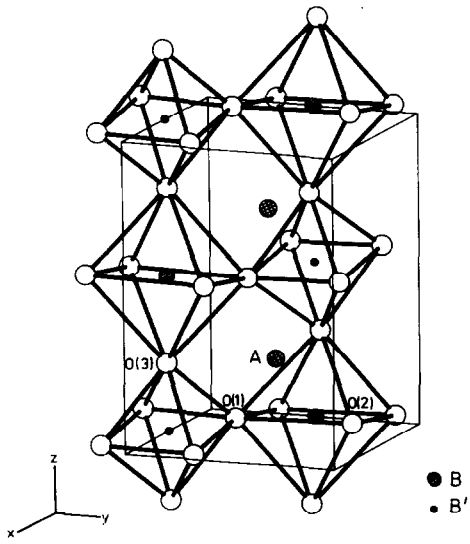

FIG. 1. The unit cell for the ordered, distorted perovskite Sr_2YRuO_6 showing the crystallographically distinct atoms.

when the diamagnetic B' cation is La^{3+} rather than Ca^{2+} (*1*, *3*).

In this paper we report our results on Sr_2YRuO_6 which has been studied in order to ascertain the extent to which a B' site occupied by Y^{3+} is involved in the magnetic superexchange pathways. Furthermore, the assignment of Ba_2LaRuO_6 and Ca_2LaRuO_6 to the $b_c < b < b_m$ region of Fig. 2 was based partly on high temperature magnetic susceptibility data (2) which gave anomalously large values for both the effective magnetic moment, and the ratio of the Curie–Weiss temperature (θ) to the Néel temperature (T_N). The Néel temperature of Sr_2YRuO_6 has not been determined previously, but a value of 3.13 μ_B has been reported for the effective magnetic moment in the paramagnetic phase (*2*). This rather low value indicates that we may be dealing with a localized $4d^3$ system ($b < b_c$) with strong second-order spin orbit coupling and we have therefore measured T_N and the ordered magnetic moment in the antiferromagnetic phase to determine if these provide any further evidence for the existence of a localized $Ru^{5+}: 4d^3$ electron system in Sr_2YRuO_6. The magnetic moment per Ru^{5+} ion was determined from powder neutron diffraction data which also allowed us to refine the crystal structure of Sr_2YRuO_6.

Experimental

Sr_2YRuO_6 was prepared by firing a pelleted stoichiometric mixture of strontium

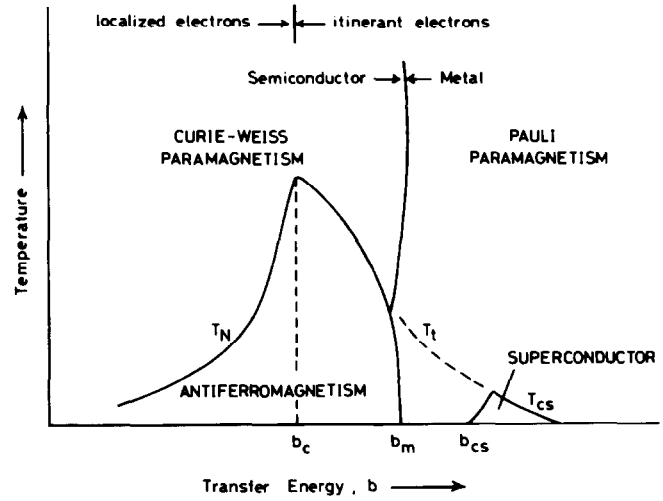

FIG. 2. Conceptual temperature vs transfer-integral phase diagram for one electron per orbital.

TABLE I

ATOMIC POSITIONS AND ISOTROPIC TEMPERATURE FACTORS FOR Sr_2YRuO_6 AT ROOM TEMPERATURE

Atom	x	y	z	B (Å^2)
Sr	0.5073(6)	0.5274(2)	0.2497(6)	0.52(2)
Y	0	½	0	0.34(3)
Ru	½	0	0	0.44(4)
O(1)	0.2339(6)	0.2036(7)	−0.0341(5)	0.65(2)
O(2)	0.3021(6)	0.7293(6)	−0.0339(5)	0.65(2)
O(3)	0.4331(6)	−0.0127(5)	0.2347(4)	0.65(2)

carbonate, yttrium sesquioxide, and ruthenium dioxide in air at 900°C for 12 hr and then for 10 days at 1200°C with regular grinding and repelleting. The reaction was carried out in a platinum crucible. Analytical electron microscopy showed that the final product was an homogeneous, single phase and the peaks in a powder X-ray diffraction pattern could be indexed using unit-cell parameters close to those reported previously (*2*, *4*).

Time-of-flight powder neutron diffraction data were collected at room temperature using the General Purpose Powder Diffractometer at the Intense Pulsed Neutron Source at Argonne National Laboratory. All subsequent analyses were performed on the data collected at $2\theta = 90°$ in order to optimize the balance between intensity and resolution. At this angle, the detectors have a channel width of 8 μsec, and the incident wavelength varies from 0.19 to 5.76 Å. The data were collected over a period of 12 hr. Constant-wavelength (1.372 Å) powder neutron diffraction data were collected at 4.2 K using the CURRAN diffractometer at AERE Harwell, England. A 2θ-step size of 0.1° was used with a monitor count of 4×10^4 neutrons per point.

The magnetic susceptibility of Sr_2YRuO_6 was measured in the temperature range 4.2–67 K with an Oxford Instruments Faraday balance. A magnetic field of 38.1 kG was used with a field gradient of 121 G cm^{-1}.

Results

The room temperature neutron diffraction data were analyzed using the Rietveld profile analysis technique (*5*), as modified for time-of-flight data by Von Dreele *et al.* (*6*). The 1198 reflections contributed to the 2190 profile points which were included in the calculation. The following scattering lengths were used $b_{Sr} = 0.69$, $b_Y = 0.79$, $b_{Ru} = 0.73$, $b_O = 0.58 \times 10^{-14}$ m. The data were best fitted in the monoclinic space group $P2_1/n$ with unit cell parameters $a = 5.7690(6)$, $b = 5.7777(6)$, $c = 8.1592(9)$ Å, and $\beta = 90.23(1)°$. Here and throughout this paper the number in brackets is the estimated standard deviation in the last figure. The final atomic coordinates and temperature factors after refinement of 16 atomic parameters and 12 profile parameters are given in Table I and the bond lengths and bond angles are presented in Table II. The observed, calculated, and difference profiles are plotted in Fig. 3. The final weighted profile R-factor was 3.37%. It should be

TABLE II

BOND LENGTHS (IN ÅNGSTROMS) AND BOND ANGLES (IN DEGREES) FOR Sr_2YRuO_6 AT ROOM TEMPERATURE

Y–O(1)	2.199(6)	Ru–O(1)	1.953(6)
Y–O(2)	2.208(6)	Ru–O(2)	1.955(6)
Y–O(3)	2.199(6)	Ru–O(3)	1.956(6)

Sr–O(1)	Sr–O(2)	Sr–O(3)
3.365(8)	2.845(8)	3.152(8)
2.786(8)	2.555(8)	2.694(8)
2.566(8)	2.822(8)	2.555(8)
2.895(8)	3.400(8)	3.239(8)

O(1)–Y–O(2)	91.9	O(1)–Ru–O(2)	90.2
O(1)–Y–O(3)	90.4	O(1)–Ru–O(3)	90.2
O(2)–Y–O(3)	90.4	O(2)–Ru–O(3)	90.5

Note. Estimated standard deviation in bond angle is 1°.

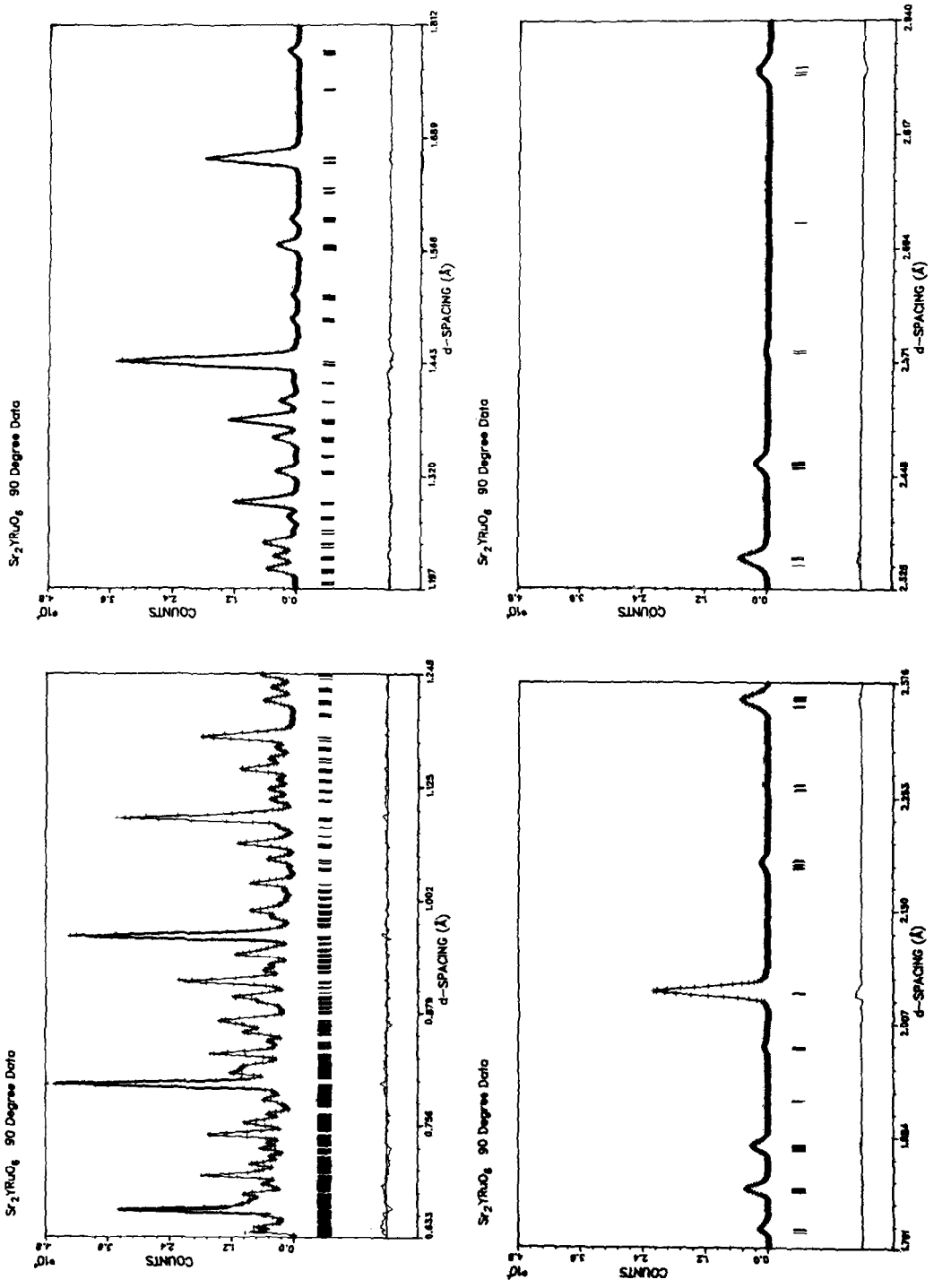

FIG. 3. The observed (+), calculated (−), and difference profiles for Sr_2YRuO_6 at room temperature. Reflection positions are marked.

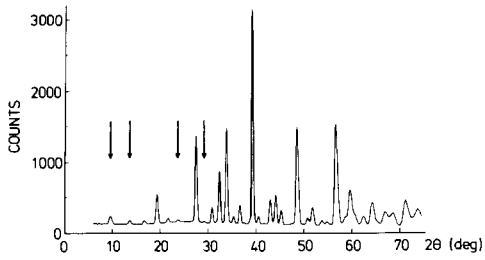

FIG. 4. The observed neutron diffraction pattern for Sr_2YRuO_6 at 4.2 K. Magnetic reflections are arrowed.

noted that the background level was refined in this analysis, rather than estimated and subtracted as is usual in constant-wavelength work. The R-value quoted is defined as

$$R_{wpr} = 100 \sum_i (w_i y_i^{obs} - c y_i^{calc})^2 \Big/ \sum_i (w_i y_i^{obs})^2$$

where w_i is the weight assigned to the ith profile point, c is the scale factor, and y_i is the *total* intensity at the ith point.

The neutron diffraction pattern recorded at 4.2 K is shown in Fig. 4. The arrowed reflections are not observed at room temperature and can be ascribed to the onset of Type I antiferromagnetic ordering. The spin arrangement in this type of magnetic structure is illustrated for the pseudocubic $\sqrt{2}a \times \sqrt{2}b \times c$ unit cell drawn in Fig. 5. It consists of ferromagnetic (001) sheets antiferromagnetically coupled along [001], the spins lying in the (001) planes as a result of dipolar interactions. In order to estimate the magnitude of the ordered magnetic moment we compared the intensity of the relatively strong, low-angle (001) magnetic peak to the intensities of several nuclear peaks, assuming a value of unity for the Ru^{5+} form factor at this low Q value ($\sin\theta/\lambda = 0.06$). The Ru^{5+} form factor is not sufficiently well known to warrant the inclusion in the analysis of the weaker magnetic peaks at higher Q values. The ordered magnetic moment was then calculated to be 1.85(10) μ_B per Ru^{5+} ion.

The low temperature magnetic susceptibility of Sr_2YRuO_6 is plotted in Fig. 6. The Néel temperature is 26 K and there is a spin-flop transition below ~12 K. The latter is a consequence of the high magnetic field used in the experiment. A similar effect was found in Ba_2LaRuO_6 (*1*).

Discussion

The results presented in Tables I and II show that the crystal structure of Sr_2YRuO_6 is very similar to those of Ba_2LaRuO_6 and Ca_2LaRuO_6 discussed above, consisting as it does of a framework of tilted, nearly regular RuO_6 and YO_6 octahedra with the large strontium ions occupying the A sites of the perovskite structure. The RuO_6 octahedra

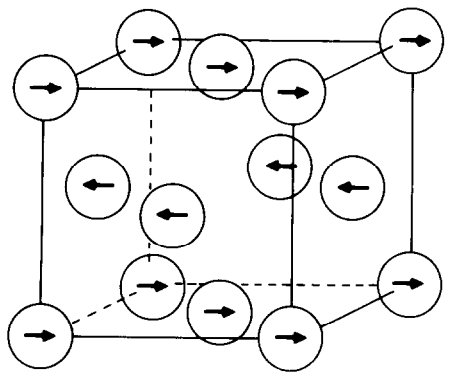

FIG. 5. The Type I magnetic unit cell of Sr_2YRuO_6. Only ruthenium ions are shown.

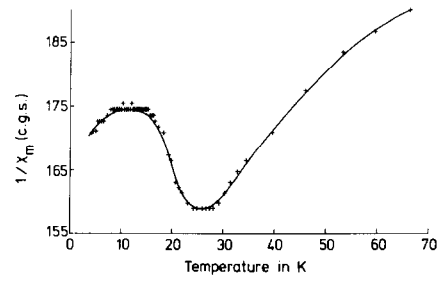

FIG. 6. The reciprocal molar magnetic susceptibility of Sr_2YRuO_6 as a function of temperature.

are particularly regular with a very small spread in both Ru–O and O–O bond lengths, as would be expected for a Ru^{5+} ion with a $^4A_{2g}$ ground state. The Ru–O bond lengths are in good agreement with those found previously (*1*). Although the Y–O bonds in the YO_6 octahedra are all very similar in length, the distortion is greater here than in the RuO_6 case, as is demonstrated by the spread in O–O distances from 3.06 to 3.17 Å. The published values (*7–12*) of six-coordinate Y–O bond lengths vary from 2.15 to 2.39 Å, and in many cases there is a considerable spread within a particular compound. Only hexakisantipyrineyttrium triiodide (*7*) contains yttrium in a nearly regular octahedron with a shorter Y–O bond distance (2.190 Å) than that found in Sr_2YRuO_6.

Very few crystal structures have been refined and published using data from a spallation source such as IPNS at Argonne and it is useful to compare GPPD and the best constant wavelength powder diffractometer in routine use, Dla at ILL Grenoble. One obvious advantage of GPPD is that data can be taken down to a *d*-spacing of ~0.6 Å, whereas Dla has a cutoff at ~1 Å when used at its normal wavelength of 1.909 Å. This gain is partly countered by the high degree of reflection overlap which occurs at low *d* values, thus making it harder to extract information from the pattern. The resolution of GPPD is slightly worse than that of Dla in the *Q* range where the latter is at its best, but GPPD retains the same high resolution over a wide range of *Q* values whereas that of Dla is strongly *Q* dependent. The e.s.d.'s on the bond lengths presented in Table II are very similar to those we would have expected from Dla data (*1*). The major disadvantage of GPPD is that data at large *d*-spacings can only be recorded on the low-resolution counter at $2\theta = 30°$. For example, the data with $2\theta < 20°$ in Fig. 4 cannot be recorded on the GPPD counter at $2\theta = 90°$; it is thus impossible to refine crystal and magnetic structures simultaneously if the former requires the use of a high resolution counter and the latter the use of data at large *d*-spacings.

The two most important antiferromagnetic exchange interactions in Sr_2YRuO_6 are likely to be the π-superexchange between nearest-neighbor Ru^{5+} ions via a Ru–O–O–Ru pathway and the σ-superexchange between next-nearest neighbors via a Ru–O–Y–O–Ru pathway. The relative strengths of these two interactions will determine the type of antiferromagnetic ordering which occurs at low temperatures. If the next-nearest neighbor interaction is much the stronger, then we expect Type II magnetic ordering where each cation has six next-nearest neighbors with antiparallel spins (*13*), but there is no net antiferromagnetic stabilization of the nearest neighbors other than by exchangestriction (*1*). As the strength of the nearest-neighbor interaction increases, the system will move to Type IIIa ordering rather than Type II. In this case eight of the nearest neighbors and two of the next-nearest neighbors are coupled antiparallel to the central ion. When the strength of the next-nearest neighbor interactions approaches zero, Type I ordering (Fig. 5) can occur. Here eight of the nearest neighbors are coupled antiferromagnetically to the central ion, as in Type IIIa, and all the next-nearest neighbors are ferromagnetically coupled.

The existence of Type I magnetic ordering in Sr_2YRuO_6 demonstrates that the Y^{3+} ions on the *B'* sites do not play a significant role in the magnetic superexchange, presumably because they do not possess the vacant, energetically accessible orbitals necessary to take part in a Ru–O–Y–O–Ru exchange pathway. As in Ca_2LaRuO_6, the dominant exchange interaction is the nearest-neighbor superexchange along the face diagonal of the pseudocubic unit cell drawn in Fig. 5. This is consistent with the strong π-superexchange expected for a d^3 ion with

half-filled t_{2g} orbitals and empty e_g orbitals. The ordered magnetic moment of 1.85 μ_B per Ru^{5+} ion is comparable to the values of 1.96 and 1.92 μ_B found in Ba_2LaRuO_6 and Ca_2LaRuO_6, respectively. The high temperature susceptibility data of Greatrex *et al.* (*2*) enable us to assign a maximum value of 1.62 to the Lande g-factor of Ru^{5+} in Sr_2YRuO_6, this value being calculated from the value of 3.13 μ_B reported for the effective magnetic moment in the paramagnetic phase. Using a g-value of 1.62, a calculation of the covalency parameter (*14*) for Sr_2YRuO_6 leads to a value of 5.5% for A_π^2, as defined by

$$S/S_0 = 1 - 4A_\pi^2$$

where S is the observed spin and S_0 is the free ion spin corrected for zero-point spin deviations (*15*). Although smaller than the values reported for Ba_2LaRuO_6 and Ca_2LaRuO_6 (1), 5.5% is larger than the values of 1.6 and 3.3% reported (*16*) for two d^3 ions from the first transition series, Cr^{3+} in $LaCrO_3$ and Mn^{4+} in $CaMnO_3$. This is predictable in view of the decreased size and increased charge of the Ru^{5+} ion. Our estimates (*1*) of the covalency parameter, A_π^2, for Ba_2LaRuO_6 and Ca_2LaRuO_6 may be too large because the high temperature μ_{eff} values for these two compounds (4.00 and 4.27 μ_B, respectively) did not permit us to make any useful estimate of the extent to which the ordered magnetic moment might be reduced from the spin-only value by second-order spin orbit coupling, and a g-value of 2 was therefore assumed in calculating A_π^2.

The location of Sr_2YRuO_6 on the T_N vs b phase diagram (Fig. 2) is less clear than that of Ca_2LaRuO_6 or Ba_2LaRuO_6, both of which have anomalously large effective magnetic moments in the paramagnetic phase and values of the ratio $\theta/T_N > 10$, this behavior being indicative of a transfer integral in the range $b_c < b < b_m$ (*1*). The effective magnetic moment of Sr_2YRuO_6 has a value below that predicted by the spin-only formula, as would be expected for a localized d^3 ion in an octahedral crystal field. However, the value of 5.5 calculated for the θ/T_N ratio is rather large fo a well-behaved, localized antiferromagnet, although clearly not as large as that found for Ba_2LaRuO_6 or Ca_2LaRuO_6. The ordered magnetic moment is as low as those found for these two compounds, but there is evidence to suggest that the moment reduction due to covalency, which is a measure of b, is smaller than was thought previously. Without data on the variation of Néel temperature with pressure we are unable to locate Sr_2YRuO_6 on Fig. 2 with any degree of confidence. However, it does seem clear that b is lower for this material than for either of those studied previously, and it may well be that the correlation splitting between the $4d^3$ and $4d^4$ configurations is large enough to give $b < b_c$ for Sr_2YRuO_6.

Acknowledgments

We are grateful to the SERC for supporting our neutron diffraction program (GR/C/04352 and GR/C/53015), to Mr. G. Proudfoot for experimental assistance at AERE Harwell, and to the Central Electricity Generating Board and St. Catherine's College Oxford for a Research Fellowship for P.D.B. Finally, we are indebted to all the staff at IPNS Argonne who helped to make our stay such a success, particularly Dr. J. Faber.

References

1. P. D. Battle, J. B. Goodenough, and R. Price, *J. Solid State Chem.* **46,** 234 (1983).
2. R. Greatrex, N. N. Greenwood, M. Lal, and I. Fernandez, *J. Solid State Chem.* **30,** 137 (1979).
3. J. B. Goodenough, "Magnetism and the Chemical Bond," Wiley, New York (1963).
4. P. C. Donohue and E. L. McCann, *Mater. Res. Bull.* **12,** 519 (1977).
5. H. M. Rietveld, *J. Appl. Crystallogr.* **2,** 65 (1969).
6. R. B. Von Dreele, J. D. Jorgensen, and C. G. Windsor, *J. Appl. Crystallogr.* **15,** 581 (1982).

7. R. W. BAKER AND J. W. JEFFERY, *J. Chem. Soc. Dalton* 229 (1974).
8. L. A. HARRIS AND H. L. YAKEL, *Acta Crystallogr.* **22,** 354 (1967).
9. B. H. O'CONNOR AND T. M. VALENTINE, *Acta Crystallogr. Sect. B* **25,** 2140 (1969).
10. H. MULLER-BUSCHBAUM, *Z. Anorg. Allg. Chem.* **358,** 138 (1968).
11. B. A. MAKSIMOV, V. V. ILYUKHIN, AND N. V. BELOV, *Sov. Phys. Crystallogr.* **11,** 583 (1967).
12. B. A. MAKSIMOV, V. V. ILYUKHIN, Y. A. KHARITONOV, AND N. V. BELOV, *Sov. Phys. Crystallogr.* **15,** 806 (1971).
13. R. A. TAHIR-KHELI, H. B. CALLEN, AND H. JARRETT, *J. Phys. Chem. Solids* **27,** 23 (1966).
14. J. HUBBARD AND W. MARSHALL, *Proc. Phys. Soc.* **86,** 561 (1965).
15. H. H. DAVIS, *Phys. Rev.* **120,** 789 (1960).
16. B. C. TOFIELD AND B. E. F. FENDER, *J. Phys. Chem. Solids* **31,** 2741 (1970).